

## Plasma sheet oscillations and their relation to substorm development: Cluster and double star TC1 case study

T. Takada<sup>a,b,\*</sup>, R. Nakamura<sup>a</sup>, Y. Asano<sup>c</sup>, W. Baumjohann<sup>a</sup>, A. Runov<sup>a</sup>, M. Volwerk<sup>a,d</sup>,  
T.L. Zhang<sup>a</sup>, Z. Vörös<sup>a,e</sup>, K. Keika<sup>a</sup>, B. Klecker<sup>d</sup>, H. Rème<sup>f</sup>, E.A. Lucek<sup>g</sup>,  
C. Carr<sup>g</sup>, H.U. Frey<sup>h</sup>

<sup>a</sup> Space Research Institute, Austrian Academy of Sciences, Schmiedlst. 6, A-8042 Graz, Austria

<sup>b</sup> Institute of Space and Astronautical Science, Japan Aerospace Exploration Agency, Yoshinodai 3-1-1, Sagami-hara 229-8510, Japan

<sup>c</sup> Tokyo Institute of Technology, Ookayama 2-12-1, Meguro, Tokyo 152-8550, Japan

<sup>d</sup> Max-Planck-Institut für extraterrestrische Physik, Postfach 1312, D-8574 Garching, Germany

<sup>e</sup> Institute of Atmospheric Physics, AS CR, 14131 Boční II 1401, Prague 4, Czech Republic

<sup>f</sup> CESR/CNRS, 9 Avenue du Colonel Roche, F-31028 Toulouse Cedex 4, France

<sup>g</sup> Imperial College, Prince Consort Road, London SW7 2BZ, UK

<sup>h</sup> Space Sciences Laboratory, University of California, 7 Gauss Way #7450, Berkeley, CA 94720-7450, USA

Received 1 November 2006; received in revised form 22 February 2007; accepted 3 April 2007

### Abstract

We examined two consecutive plasma sheet oscillation and dipolarization events observed by Cluster in the magnetotail, which are associated with a pseudo-breakup and a small substorm monitored by the IMAGE spacecraft. Energy input from the solar wind and an associated enhancement of the cross-tail current lead to current sheet thinning and plasma sheet oscillations of 3–5 min periods, while the pseudo-breakups occur during the loading phase within a spatially limited area, accompanied by a localized dipolarization observed by DSP TC1 or GOES 12. That is, the so-called “growth phase” is a preferable condition for both pseudo-breakup and plasma sheet oscillations in the near-Earth magnetotail. One of the plasma sheet oscillation events occurs before the pseudo-breakup, whereas the other takes place after pseudo-breakup. Thus there is no causal relationship between the plasma sheet oscillation events and pseudo-breakup. As for the contribution to the subsequent small substorm, the onset of the small substorm took place where the preceding plasma sheet oscillations can reach the region.

© 2007 COSPAR. Published by Elsevier Ltd. All rights reserved.

**Keywords:** Magnetosphere; Plasma sheet; Substorm; Pseudo-breakup; Oscillation

### 1. Introduction

It is well known that the plasma sheet often oscillates in the magnetotail (e.g., Sergeev et al., 1998). Past studies reported some types of oscillation such as tail flapping (e.g., Fairfield et al., 1981), kink-like flapping (e.g., Volwerk et al., 2003; Runov et al., 2003, 2006; Sergeev et al., 2004; Zhang et al., 2005), eigen-oscillations (e.g., Louarn et al., 2004; Fruit et al., 2004) and compressional modes

(e.g., Volwerk et al., 2004). In the statistics of large-amplitude flapping motions, Sergeev et al. (2006) reported that kink-like flapping is preferentially observed during the substorm expansion phase but may also occur in any phase of a substorm including quiet conditions. Although the azimuthal propagation of kink-like plasma sheet waves (Runov et al., 2005) suggests the generation mechanism of a flow-associated instability rather than ion drift-associated instabilities, such plasma sheet oscillations are observed both during flow and non-flow intervals. The generation mechanism is still controversial. On the other hand, the plasma sheet can be locally thinned due to the oscilla-

\* Corresponding author. Tel.: +81 42 759 8168; fax: +81 42 759 8456.  
E-mail address: [taku.takada@oeaw.ac.at](mailto:taku.takada@oeaw.ac.at) (T. Takada).

tions (e.g., Karimabadi et al., 2003), which is a good condition for the current sheet instability responsible for substorm onset. Understanding the relationship between plasma sheet oscillations and global reconfigurations of the magnetosphere may give us keys to confirm the generation mechanism and the contribution to the substorm development.

A substorm is one of the most dominant phenomena in the magnetotail and has sometimes consecutive multiple onsets. Comparing the solar wind parameters with geomagnetic activities, Mishin et al. (2001) investigated two successive substorm events, where the first one is often smaller and sometimes rather more like a pseudo-breakup (e.g., Pulkkinen et al., 1998). The first onset occurred during southward Interplanetary Magnetic Field (IMF) and the second onset occurred at a northward turning of IMF. The reconnection does not expand to the lobe region at the first onset and does expand to the lobe for the second onset due to the difference of dayside and nightside reconnection rates. Russel (2000) later extends this idea to a more general one, i.e., the northward turning of the IMF triggers substorms since the IMF turning suppresses the distant neutral lines. However, it is still unknown how much the magnetotail condition affects the double onset substorm and vice versa.

In this paper we report the Cluster and Double Star Program (DSP) “Tan Ce 1” (TC1) conjunction events (e.g., Takada et al., 2006) where plasma sheet oscillations and dipolarization are observed in the magnetotail, associated with a pseudo-breakup and a small substorm measured by the Imager for Magnetopause-to-Aurora Global Exploration (IMAGE) spacecraft. The generation mechanism and the contribution of the plasma sheet oscillations to the substorm development are discussed, taking into account the order of the above phenomena and their spatial extent. We mainly use data obtained by the FluxGate Magnetometer (FGM) instrument on Cluster (Balogh et al., 2001) and on TC1 (Carr et al., 2005), and the Composition and Distribution Function analyser (CODIF) and Hot Ion Analyser (HIA) of the Cluster Ion Spectrometry experiment (CIS) (Rème et al., 2001) onboard Cluster. Throughout the paper the Geomagnetic Solar Magnetospheric (GSM) coordinate system is used unless specified otherwise. The Wideband Imaging Camera (WIC) of the Far Ultra-Violet imager (FUV) onboard IMAGE provides an auroral image for 5–10 s in each 2 min spin period (Mende et al., 2000).

## 2. Event overview

On 3 September 2004 Cluster and DSP TC1 provide a radially aligned observation in the near-Earth magnetotail close to the midnight meridian as shown in Fig. 1i and j. Due to the Cluster polar orbit, it is rare that both spacecraft stayed simultaneously in the plasma sheet. This event is one of seven events when both spacecraft was in the plasma sheet in 2004 summer and aurora onsets were detected by IMAGE spacecraft. Auroral images taken by IMAGE WIC show two pairs of a pseudo-breakup fol-

lowed up by a small substorm shown in Panel 1. Each row corresponds to the three snapshots of the first pseudo-breakup, the first small substorm, the second pseudo-breakup, and the second small substorm, respectively. In Fig. 1d and Panel 1, onsets of those auroral brightening are marked as p1 at ~0108 UT, s1 at ~0131 UT, p2 at ~0212 UT and s2 at ~0231 UT. Since the last small substorm originally appeared at the dusk side and then developed toward midnight, the s2' at 0237 UT is also marked as time when the auroral brightening reached the spacecraft position. The onset timing ambiguities are within a spin period, which are marked as the gray shaded area in Fig. 1d. In Fig. 1a, the IMF  $B_Z$  of ACE at (223, 4, -2)  $R_E$  and of Geotail at (20, 2, 4)  $R_E$  show the large inconsistency between the two spacecraft especially until 0230 UT, which may suggest a localized IMF structure. Geotail is located closer to the Earth and the measurements are more plausible for the IMF which actually reaches the Earth's magnetosphere. Note that the Geotail data was sometimes affected by the foreshock (e.g., Kaymaz and Sibeck, 2001) and such intervals are removed in Fig. 1a. Two of the pseudo-breakups occur during the foreshock interval observed by Geotail, i.e., 0054–0120 UT and 0200–0217 UT respectively, while ACE observes northward IMF (p1) and southward IMF (p2). Small substorms, where quick look  $AL$  index are around -100 nT, occur during the weak southward IMF (s1) observed by Geotail and at northward turning (s2).

In the plasma sheet Cluster at (-18, -1, 0)  $R_E$  observed the oscillations before/around the first pseudo-breakup and after the second pseudo-breakup, which are shown as shaded areas in Fig. 1e. Interestingly, these oscillation intervals correspond to the interval of enhanced  $V_Y$ , i.e., enhancement of duskward ion drift, shown also by gray shaded areas in Fig. 1f. At the first small substorm onset, Cluster observed earthward beams near the plasma sheet-lobe boundary at 0128 UT and then earthward bulk flows at 0132 UT after plasma sheet expansion, accompanied by a bipolar  $B_Z$ . At the second small substorm onset, Cluster observed earthward bulk flows at 0233 UT with a bipolar  $B_Z$ . Detailed studies of the dipolarization transition during these small substorms are performed (Fazakerley, A.N., private communication, 2006). In Fig. 1g, the magnetic field strength in the lobe is shown, calculated from the magnetic field and proton pressures assuming pressure balance. The  $B_L$  tends to decrease after the auroral activations: during 0110–0120 UT after the first pseudo-breakup, 0128–0140 UT after the first small substorm, 0210–0215 UT after the second pseudo-breakup, and 0235–0255 UT after the second small substorm. This is considered to be due to the energy release for auroral activations and/or plasmoids. On the other hand,  $B_L$  increases during the plasma sheet oscillations and ion drift enhancement, i.e., at 0050–0110 UT and 0215–0235 UT although the intervals do not correspond exactly to each other. This  $B_L$  increase is a typical feature of the growth phase, even if the IMF condition is not clear in this event.

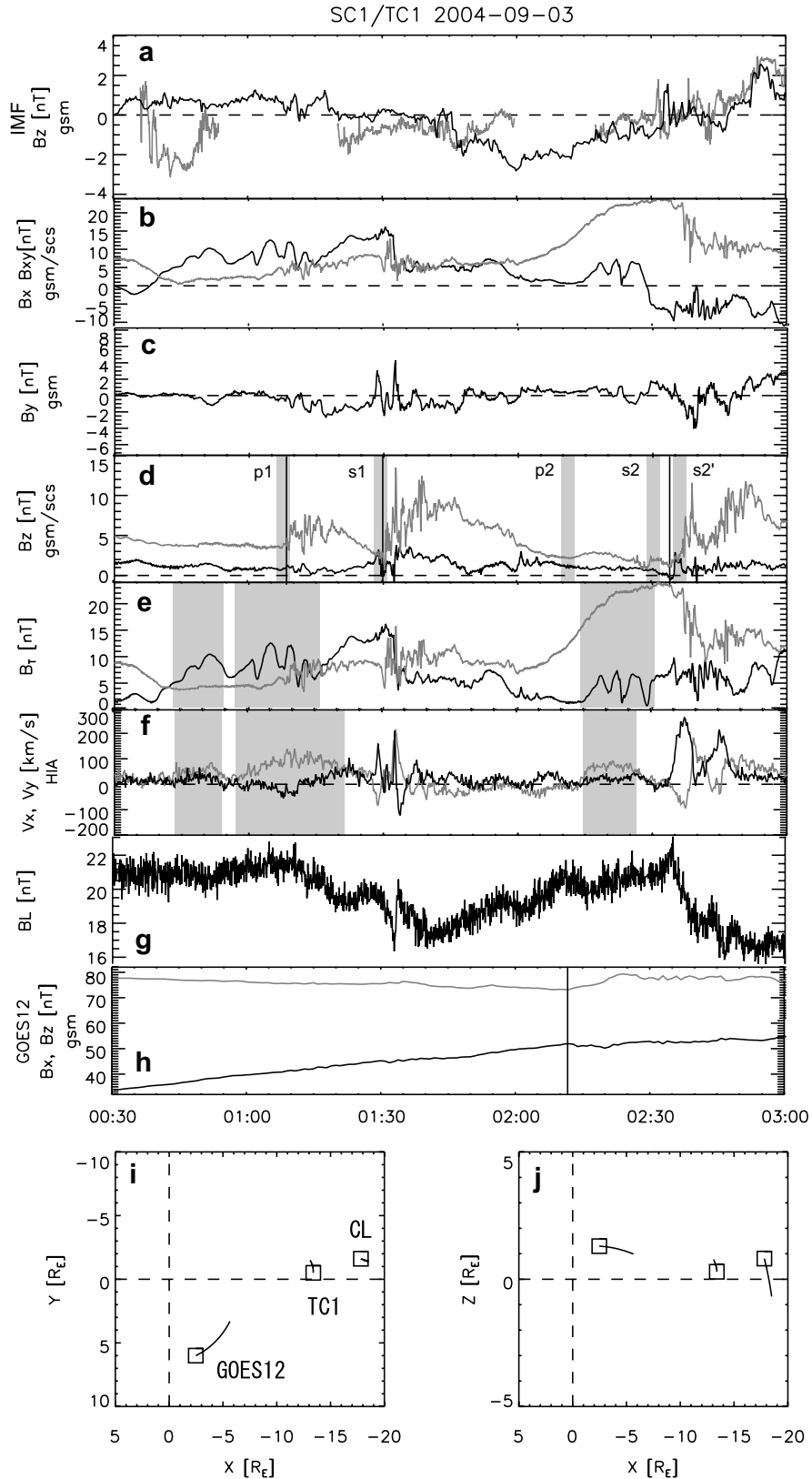
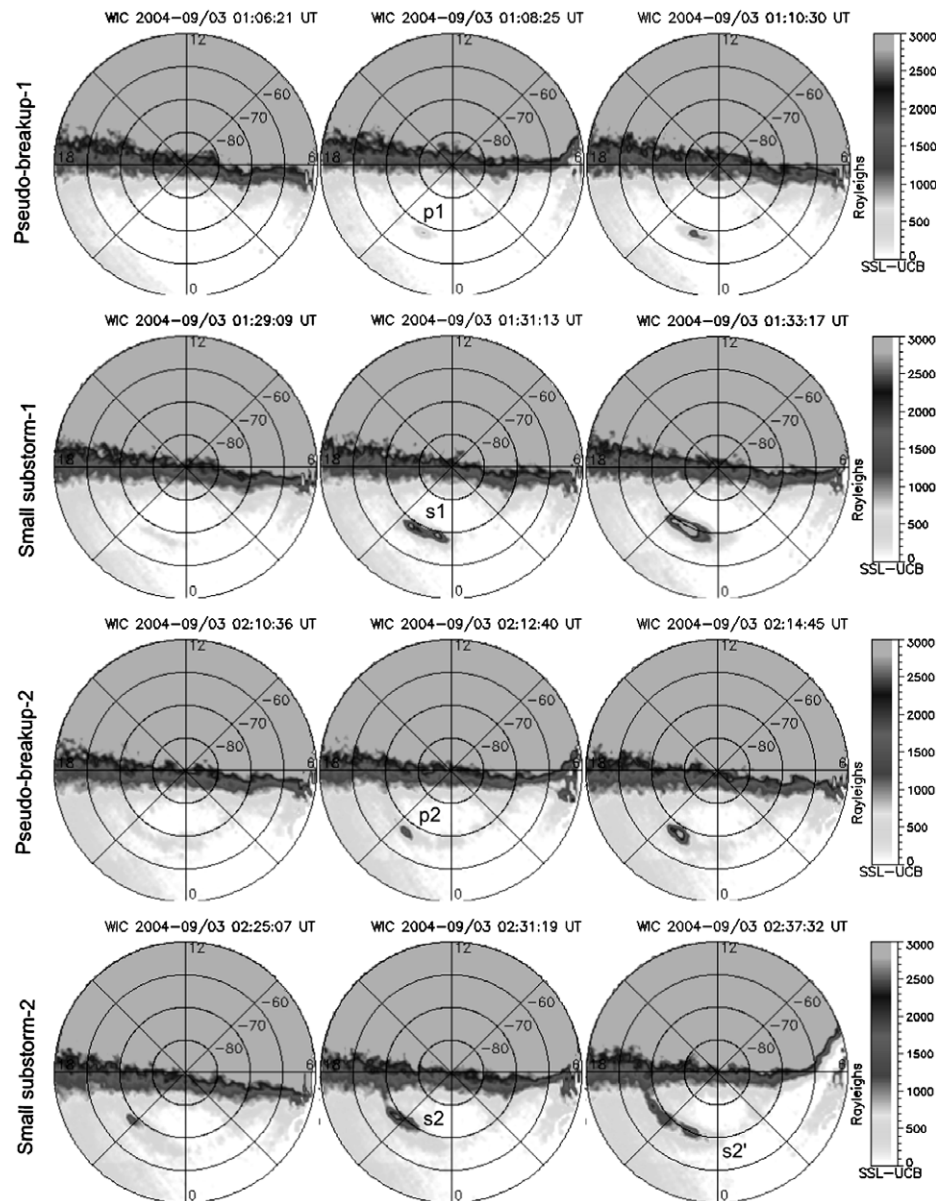


Fig. 1. Overview of spacecraft data on 3 September 2004. From top to bottom: (a) time-shifted IMF  $B_z$  observed from ACE (black) and Geotail (gray) onto  $X \sim 10 R_E$ , Cluster SC1 (black) and DSP TC1 (gray) data of (b–d) three component of magnetic field, (e) total magnetic field, (f)  $X$  (black) and  $Y$  (gray) component of ion velocity on SC1, (g) lobe magnetic field,  $B_L$ , calculated from magnetic field and proton pressure assuming the pressure balance, (h)  $B_x$  (black) and  $B_z$  (gray) component of GOES12, and spacecraft orbits on (i)  $X$ – $Y$  plane and (j)  $X$ – $Z$  plane. Start points are marked as rectangles. Black vertical lines show the dipolarization fronts in (d and h). Gray shaded area show the auroral onset intervals detected by IMAGE FUV/WIC in (d), plasma sheet oscillation events in (e), and the enhancement of duskward ion drift in (f).



Panel 1. Auroral images in MLAT-MLT maps obtained by the IMAGE FUV/WIC in the southern hemisphere. Each row shows the consecutive snapshots, from top to bottom, during the first pseudo-breakup, the first small substorm, the second pseudo-breakup, and the second small substorm. Each aurora brightening at onset is marked as p1, s1, p2 and s2 (see text), which corresponds to the one in Fig. 1d.

TC1 was located close to the Earth at  $(-13, -1, 1) R_E$  and observed three dipolarizations around the first pseudo-breakup, the first small substorm and the second small substorm events shown by vertical lines in Fig. 1d. Around the second pseudo-breakup, TC1 shows the gradual stretching of magnetotail like in the growth phase, which also corresponds to the interval of southward IMF and the two-step  $B_L$  increase. TC1 was in eclipse until 0135 UT and the spacecraft spin-plane and spin-axis components of the magnetic field are shown as  $B_{XY}$  ( $= \sqrt{B_X^2 + B_Y^2}$ ) and  $B_Z$  in SCS (Spacecraft-Sun Coordinate System) which is more or less similar to GSM  $XY$  and  $Z$ . At least the large dipolarization feature can be detected

even in SCS coordinates. Using the non-eclipse period after 0135 UT, the dipolarization was detected both in GSM and SCS coordinates (not shown). One of the geosynchronous spacecraft, GOES 12, was approaching the pre-midnight sector during this interval and observed the dipolarization at 0212 UT around the second pseudo-breakup shown by a vertical line in Fig. 1h. As a result, the two pseudo-breakups are associated with the localized dipolarizations and the two small substorms are associated with more global dipolarizations, which develop down to the Cluster position. As for the plasma sheet oscillations, TC1 seems to observe weak oscillations after 0100 UT, although the quantitative confirmation is difficult due to the eclipse. On the other hand, TC1 does not have to observe the

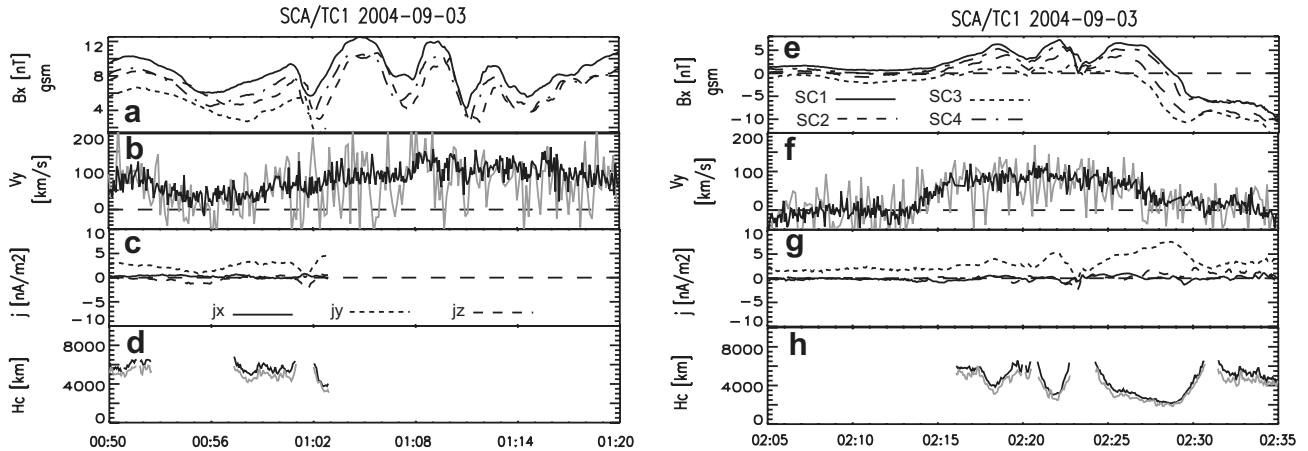


Fig. 2. Two of plasma sheet oscillation intervals on 3 September 2004: (a and e)  $B_X$  components of four Cluster spacecraft, (b and f)  $Y$  component of ion velocity onboard SC1 (black) and proton velocity onboard SC4 (gray), (c and g) three components of curlometer current,  $j_{xyz}$ , and (d and h) the estimated half-thickness of the current sheet using  $B_L$  calculated from SC1 (black) and SC4 (gray).

plasma sheet oscillation anymore during the second oscillation interval because it goes outside the plasma sheet.

In Fig. 2a and d,  $B_X$  of all Cluster spacecraft clearly shows the plasma sheet oscillations of 3–5 min periods. Using the four spacecraft timing analysis (Harvey, 1998) with a cross-correlation of  $B_X$  (first case) and a timing of  $B_X$  minima (second case), the propagation velocity of the plasma sheet oscillations is determined as  $V_p \sim (-10, 40, -15)$  km/s before the first pseudo-breakup (p1) and  $V_p \sim (0, 55, -40)$  km/s after the second pseudo-breakup (p2). As a result, the wavelength is roughly estimated as 1.5–2.5  $R_E$  in  $Y$  direction, which is slightly shorter than the previous studies: 3  $R_E$  by Runov et al. (2003) and 4  $R_E$  by Zhang et al. (2005). In the first case the plasma sheet oscillates first in the midnight sector and the waves propagate duskward. Then the pseudo-breakup (p1) occurs  $\sim 10$  min later at the dusk side. Taking into account the propagation velocity and the Cluster position, these oscillations should reach  $\sim 2230$  MLT at the pseudo-onset with a constant propagation velocity. The arrival point seems to be on the auroral region and consistent with the expectation that the plasma sheet oscillations can produce some instability in the region where the pseudo-breakup is going to occur. On the other hand, the plasma sheet oscillations occur at midnight after the second pseudo-breakup (p2) and then propagate toward the pseudo-breakup region. Note that if we assume that the propagation is like a rarefaction type wave, the short time delay between the pseudo-breakup and the plasma sheet oscillations is inconsistent with the propagation velocity. This may suggest no relationship between the pseudo-breakup and the plasma sheet oscillations. In Fig. 2, during the plasma sheet oscillation events, the cross-tail current,  $j_Y$ , which is calculated by the curlometer technique (Chanteur, 1998), enhances and the duskward ion drift,  $V_Y$  also enhances simultaneously as shown before. The estimated half-thickness of the current sheet,  $H_c$ , which is calculated from the Ampère's law, i.e.,  $j_Y = B_L H_c / \mu_0$ , decreases during the plasma sheet

oscillations. This current sheet thinning is also a typical feature in the growth phase.

### 3. Generation and contribution of the plasma sheet oscillations

In Fig. 3, the order and the spatial extent of some phenomena in each region are summarized. In order to compare with the auroral images, the spacecraft positions are mapped onto the ionospheric plane using the T96 model (Tsyganenko, 1995). In the first event, the plasma sheet oscillations are first observed with an enhancement of the duskward ion drift and propagate toward the pseudo-breakup region. Ten minutes later, when the oscillation front (second shaded area in Fig. 2e) can reach the region, the pseudo-breakup occurs in the slightly duskward side with the dipolarization at TC1. The position of the oscillation front is calculated from the delay time and the propagation speed estimated with the Cluster timing analysis and then mapped by T96. Furthermore, when the oscillation front reaches the more duskward region of the aurora 20 min after the pseudo-breakup, the auroral brightening starts to develop associated with the small substorm, where Cluster and TC1 observe the BBFs and dipolarization, respectively. It is well known that the BBF has a very confined spatial scale on the  $Y$ - $Z$  plane less than 3  $R_E$  (Nakamura et al., 2005). In the second event, the pseudo-breakup first occurs at the dusk sector, accompanied by duskward ion drift enhancements, while TC1 shows the stretching of the magnetotail. After the pseudo-breakup the Cluster spacecraft start to observe the duskward plasma sheet oscillations. At last the onset of a small substorm occurs, accompanied by the BBFs at Cluster and the dipolarization at TC1, close to the local time that the oscillation fronts can reach.

The two plasma sheet oscillation events are observed during the duskward ion drift enhancements. The duskward ion flows are very common around midnight and also



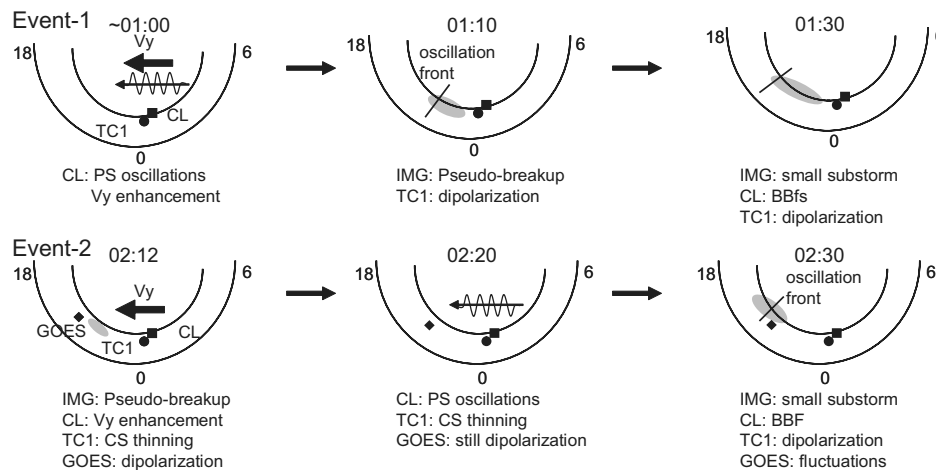


Fig. 3. Schematic snapshots on the ionospheric plane during the interval from the first pseudo-breakup to the first small substorm (top) and from the second pseudo-breakup to the second small substorm (bottom). The position of the spacecraft and the plasma sheet oscillation front are mapped by the T96 (see the text in detail).

at the dusk side and the diamagnetic drift becomes larger than the  $\mathbf{E} \times \mathbf{B}$  drift especially around the midnight meridian (e.g., Hori et al., 2000). The diamagnetic drift is also known to be enhanced during the growth phase (Wang et al., 2004) and southward IMF (Wang et al., 2006). In the first pseudo-breakup event it is not clear whether the IMF is southward as discussed in the previous section, but an enhancement of total pressure and the duskward ion drift may suggest that the situation is like a growth phase. On the other hand, the second pseudo-breakup occurs during southward IMF, which is consistent with the increase of the total pressure and the stretching of the magnetotail at TC1. During southward IMF, the solar wind energy is loaded into the whole of the magnetosphere, which leads to an enhancement of the total pressure, the pressure gradient and the diamagnetic ion drift. The enhancement of the diamagnetic drift can increase the probability for some mechanisms of plasma sheet oscillations like Kelvin-Helmholtz waves (e.g., Yoon et al., 1996) and/or the ion-ion kink waves (e.g., Karimabadi et al., 2003). Actually, the simultaneous observation of the plasma sheet oscillations and the current sheet thinning may be explained as the thinning by the kinking current sheet (e.g., Karimabadi et al., 2003). On this event, even if Cluster is located slightly downward of the midnight meridian, both plasma sheet oscillations propagate duskward, which is preferred by the above two mechanisms. As a result, these events may produce the duskward propagating waves by a classical mechanism during the growth phase or even during the small activities if the activation does not expand globally.

In both cases the pseudo-breakup precedes the small substorm and this type of substorms is often reported (e.g., Koskinen et al., 1993; Nakamura et al., 1994). As shown by Ohtani et al. (1993), the pseudo-breakups in this study are associated with a dipolarization, which is more

localized than in the cases of the small substorms. As in the case of Mishin et al. (2001), the following small substorm seems to occur at higher latitudes, i.e., more distant magnetotail, where the plasma sheet had oscillated and the current sheet had become thinner during the pseudo-breakup. It is also interesting to note that the propagating oscillations may reach the onset region of small substorm if it has not been suppressed. Actually, the dusk edge of the onset regions of small substorm shift duskward from the onset of the pseudo-breakup as shown in Panel 1. The shifted locations of the aurora brightening are consistent with the direction of ion drift and the plasma sheet oscillations in both events. Thus there seems to be some relationship between the pre-condition of plasma sheet and the coming auroral activation, but the quantitative study for the plasma sheet pre-condition may be necessary to understand the following auroral development.

#### 4. Summary

Using observations by Cluster, DSP TC1, and GOES 12, we examined two consecutive plasma sheet oscillation and dipolarization events in the magnetotail, each associated with a pseudo-breakup and a small substorm monitored by IMAGE FUV/WIC. While in the inner magnetosphere DSP TC1 or GOES 12 spacecraft observes the dipolarization at the onset of the pseudo-breakup, Cluster spacecraft see the plasma sheet oscillations in the midnight tail. Combining the solar wind data of ACE and Geotail it is expected that the energy input from the solar wind and an associated enhancement of the cross-tail current lead to the plasma sheet oscillations of 3–5 min periods with a wavelength of 1.5–2.5  $R_E$  in  $Y$  and the current sheet thinning. At that time, the pseudo-breakups occur during the loading phase within a spatially limited area, accompanied by a localized dipolarization. That is,

the so-called “growth phase” is a preferable condition for both the pseudo-breakup and the plasma sheet oscillations.

As for the plasma sheet oscillations, timing analysis of the data from the four Cluster spacecraft shows the duskward propagation of several tens of km/s in both cases. However, the two plasma sheet oscillation events occur before and after the pseudo-breakup, which may suggest that there is no causal relationship between the plasma sheet oscillations and the pseudo-breakup. Taking into account the propagation direction/speeds and the auroral spatial scale of the following small substorm, the plasma sheet oscillations can reach the onset region and may contribute to some instability in the plasma sheet.

## Acknowledgements

We thank U. Auster, H.-U. Eichelberger, V. Duma, J. Gloag, T. Oddy, E. Georgescu, G. Laky, and K.-H. Fornacon for making the Double Star TC1 FGM data available. The ACE spacecraft data are provided by N. Ness (Bartol Research Institute) and D. J. McComas (SWRI), and available on CDAWeb. Geotail magnetic field and plasma data were provided by T. Nagai and T. Mukai through DARTS at the Institute of Space and Astronautical Science (ISAS) in Japan. GOES 12 magnetic field data were provided by H. Singer at NOAA/SEC and also available on CDAWeb. WDC for Geomagnetism, Kyoto provides  $AL$  and  $D_{st}$  indices. The work by M. Volwerk is financially supported by the German Bundesministerium für Bildung und Forschung and the Zentrum für Luft- und Raumfahrt under contract 50 OC 0104. A part of work at IWF is supported by INTAS grant 03-51-3738.

## References

- Balogh, A., Carr, C.M., Acuna, M.H., et al. The Cluster magnetic field investigation: overview of in-flight performance and initial results. *Ann. Geophys.* 19, 1207–1217, 2001.
- Carr, C., Brown, P., Zhang, T.L., et al. The Double Star magnetic field investigation: instrument design, performance and highlights of the first year's observations. *Ann. Geophys.* 23, 2713–2732, 2005.
- Chanteur, G. Spatial interpolation for four spacecraft: theory, in: Paschmann, G., Daly, P. (Eds.), *Analysis Methods for Multi-Spacecraft Data*. ESA, Noordwijk, pp. 349–369, 1998.
- Fairfield, D.H., Hones Jr., E.W., Meng, C.-I. Multiple crossings of a very thin plasma sheet in the Earth's magnetotail. *J. Geophys. Res.* 86, 11189–11200, 1981.
- Fruit, G., Louarn, P., Budnik, E., et al. On the propagation of low-frequency fluctuations in the plasma sheet: 2. characterization of the MHD eigenmodes and physical implications. *J. Geophys. Res.* 109, A03217, doi:10.1029/2003JA01022, 2004.
- Harvey, C.C. Spatial gradients and volumetric tensor, in: Paschmann, G., Daly, P. (Eds.), *Analysis Methods for Multi-Spacecraft Data*. ESA, Noordwijk, pp. 307–322, 1998.
- Hori, T., Maezawa, K., Saito, Y., et al. Average profile of ion flow and convection electric field in the near-Earth plasma sheet. *Geophys. Res. Lett.* 27, 1623–1626, 2000.
- Karimabadi, H., Pritchett, P.L., Daughton, W., et al. Ion-ion kink instability in the magnetotail: 2. three-dimensional full particle and hybrid simulations and comparison with observations. *J. Geophys. Res.* 108, 1401(A11), doi:10.1029/2003JA01010, 2003.
- Kaymaz, Z., Sibeck, D.G. Correlating near-Earth interplanetary magnetic fields: foreshock effects. *J. Geophys. Res.* 106, 18599–18613, 2001.
- Koskinen, H.E.J., Lopez, R.E., Pellinen, R.J., et al. Pseudobreakup and substorm growth phase in the ionosphere and magnetosphere. *J. Geophys. Res.* 98, 5801–5813, 1993.
- Louarn, P., Fruit, G., Budnik, E., et al. On the propagation of low-frequency fluctuations in the plasma sheet: 1. cluster observations and magnetohydrodynamic analysis. *J. Geophys. Res.* 109, A03216, doi:10.1029/2003JA01022, 2004.
- Mende, S.B., Heeterds, H., Frey, H.U., et al. Far ultraviolet imaging from the IMAGE spacecraft: 3. spectral imaging of Lyman-alpha and OI 135.6 nm. *Space Sci. Rev.* 91, 287–318, 2000.
- Mishin, V.M., Saifudinova, T., Bazarzhapov, A., et al. Two distinct substorm onsets. *J. Geophys. Res.* 106, 13105–13118, 2001.
- Nakamura, R., Baker, D.N., Yamamoto, T., et al. Particle and field signatures during pseudobreakup and major expansion onset. *J. Geophys. Res.* 99, 207–221, 1994.
- Nakamura, R., Baumjohann, W., Moukik, C., et al. Multi-point observation of the high-speed flows in the plasma sheet. *Adv. Space Res.* 36, 1444–1447, doi:10.1016/j.asr.2005.05.10, 2005.
- Ohtani, S., Anderson, B.J., Sibeck, D.G., et al. A multisatellite study of a pseudo-substorm onset in the near-Earth magnetotail. *J. Geophys. Res.* 98, 19355–19367, 1993.
- Pulkkinen, T.I., Baker, D.N., Wiltberger, M., et al. Pseudobreakup and substorm onset: observations and MHD simulations compared. *J. Geophys. Res.* 103, 14847–14854, 1998.
- Rème, H., Aoustin, C., Bosqued, J.M., et al. First multispacecraft ion measurements in and near the Earth's magnetosphere with the identical Cluster ion spectrometry (CIS) experiment. *Ann. Geophys.* 19, 1303–1354, 2001.
- Runov, A., Nakamura, R., Baumjohann, W., et al. Cluster observation of a bifurcated current sheet. *Geophys. Res. Lett.* 30, 1036, doi:10.1029/2002GL01613, 2003.
- Runov, A., Sergeev, V.A., Baumjohann, W., et al. Electric current and magnetic field geometry in flapping magnetotail current sheets. *Ann. Geophys.* 23, 1391–1403, 2005.
- Runov, A., Nakamura, R., Baumjohann, W. Multi-point study of the magnetotail current sheet. *Adv. Space Res.* 38, 85–92, doi:10.1016/j.asr.2004.09.02, 2006.
- Russel, C.T. How northward turnings of the IMF can lead to substorm expansion onsets. *Geophys. Res. Lett.* 27, 3257–3259, 2000.
- Sergeev, V., Angelopoulos, V., Carlson, C., et al. Current sheet measurements within a flapping plasma sheet, *J. Geophys. Res.* 103, 9177–9188, 1998.
- Sergeev, V., Runov, A., Baumjohann, W., et al. Orientation and propagation of current sheet oscillations. *Geophys. Res. Lett.* 31, L05807, doi:10.1029/2003GL01934, 2004.
- Sergeev, V.A., Sormakov, D.A., Apatenkov, S.V., et al. Survey of large-amplitude flapping motions in the midtail current sheet. *Ann. Geophys.* 24, 2015–2024, 2006.
- Takada, T., Nakamura, R., Baumjohann, W., et al. Do BBFs contribute to the inner magnetosphere dipolarization. *Geophys. Res. Lett.* 33, L21109, doi:10.1029/2006GL02744, 2006.
- Tsyganenko, N.A. Modeling the Earth's magnetospheric magnetic field confined within a realistic magnetopause. *J. Geophys. Res.* 100, 5599–5612, 1995.
- Volwerk, M., Glassmeier, K.-H., Runov, A., et al. Kink mode oscillation of the current sheet. *Geophys. Res. Lett.* 30, 1320, doi:10.1029/2002GL01646, 2003.
- Volwerk, M., Baumjohann, W., Glassmeier, K.-H., et al. Compressional waves in the Earth's neutral sheet. *Ann. Geophys.* 22, 303–315, 2004.
- Wang, C.-P., Lyons, L.R., Nagai, T., et al. Midnight radial profiles of the quiet and growth-phase plasma sheet: the Geotail

- observations. *J. Geophys. Res.* 109, A12201, doi:[10.1029/2004JA01059](https://doi.org/10.1029/2004JA01059), 2004.
- Wang, C.-P., Lyons, L.R., Weygand, J.M., et al. Equatorial distributions of the plasma sheet ions, their electric and magnetic drifts, and magnetic fields under different interplanetary magnetic field  $B_Z$  conditions. *J. Geophys. Res.* 111, A04215, doi:[10.1029/2005JA01154](https://doi.org/10.1029/2005JA01154), 2006.
- Yoon, P.H., Drake, J.F., Lui, A.T.Y. Theory and simulation of Kelvin-Helmholtz instability in the geomagnetic tail. *J. Geophys. Res.* 101, 27327–27339, 1996.
- Zhang, T.L., Nakamura, R., Volwerk, M., et al. Double Star/Cluster observation of neutral sheet oscillations on 5 August 2004. *Ann. Geophys.* 23, 2909–2914, 2005.